

Deep-learning-assisted microscopy with ultraviolet surface excitation for rapid slide-free histological imaging: supplement

ZHENGHUI CHEN, WENTAO YU, IVY H. M. WONG, AND TERENCE T. W. WONG*

Department of Chemical and Biological Engineering, The Hong Kong University of Science and Technology, Clear Water Bay, Kowloon, Hong Kong, China

**ttwwong@ust.hk*

This supplement published with The Optical Society on 1 September 2021 by The Authors under the terms of the [Creative Commons Attribution 4.0 License](#) in the format provided by the authors and unedited. Further distribution of this work must maintain attribution to the author(s) and the published article's title, journal citation, and DOI.

Supplement DOI: <https://doi.org/10.6084/m9.figshare.16553847>

Parent Article DOI: <https://doi.org/10.1364/BOE.433597>

Deep-learning-assisted microscopy with ultraviolet surface excitation for rapid slide-free histological imaging: supplemental document

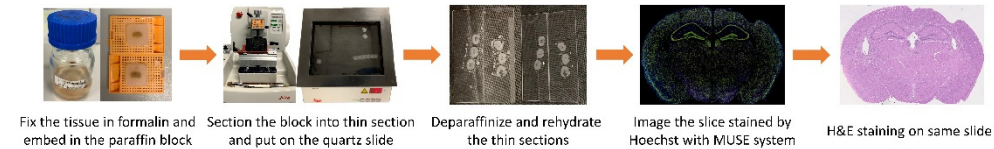


Fig. S1. Procedure for obtaining MUSE and H&E-stained images of thin mouse brain slices. A fresh mouse brain is formalin-fixed and paraffin-embedded in a block. Then, the paraffin block is sectioned and put on a quartz slide. After deparaffinization and rehydration, the tissue sample is stained with Hoechst and imaged by the MUSE system. To get the corresponding histological image, H&E staining is added on the same slice and viewed using a bright-field microscope.

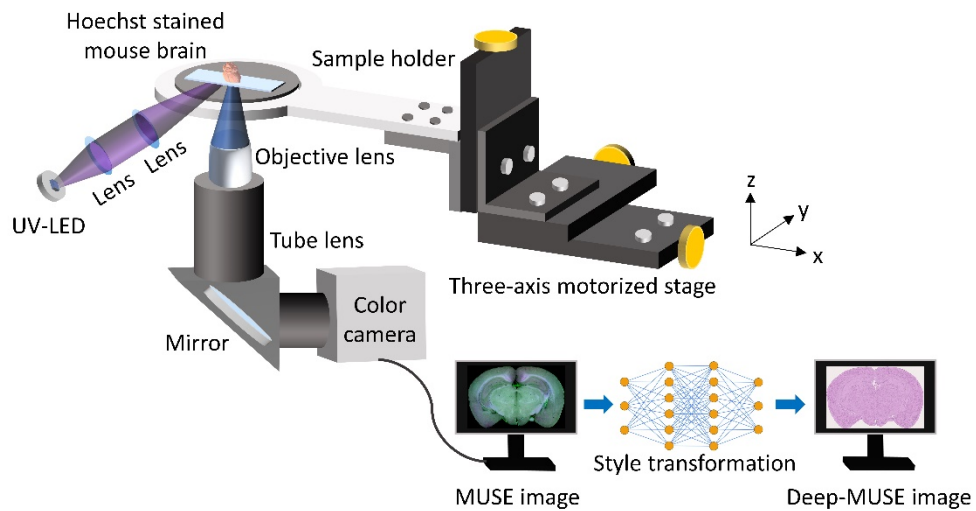
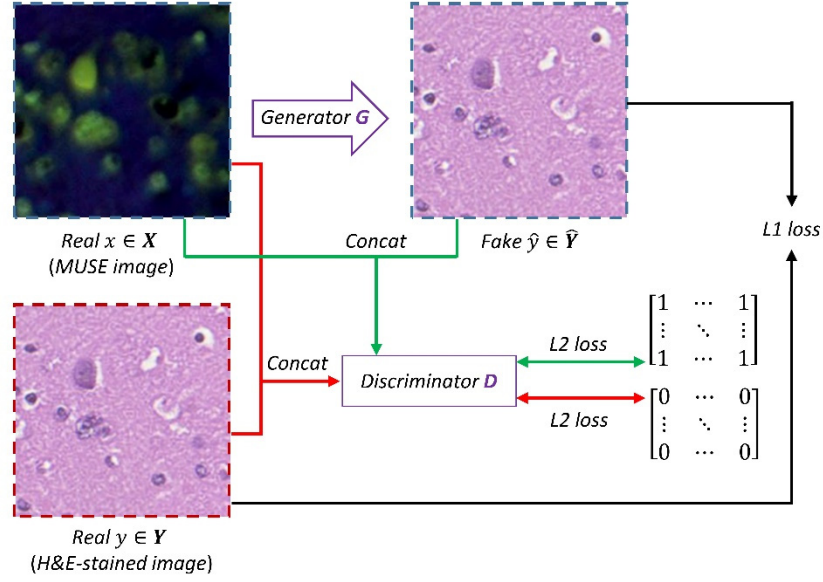


Fig. S2. Schematic of the MUSE imaging system integrated with a deep learning algorithm for rapid slide-free histological imaging. The optical configuration of the MUSE imaging system and style transformation from a MUSE image to a Deep-MUSE image that is comparable to a standard H&E-stained histological image.

A



B

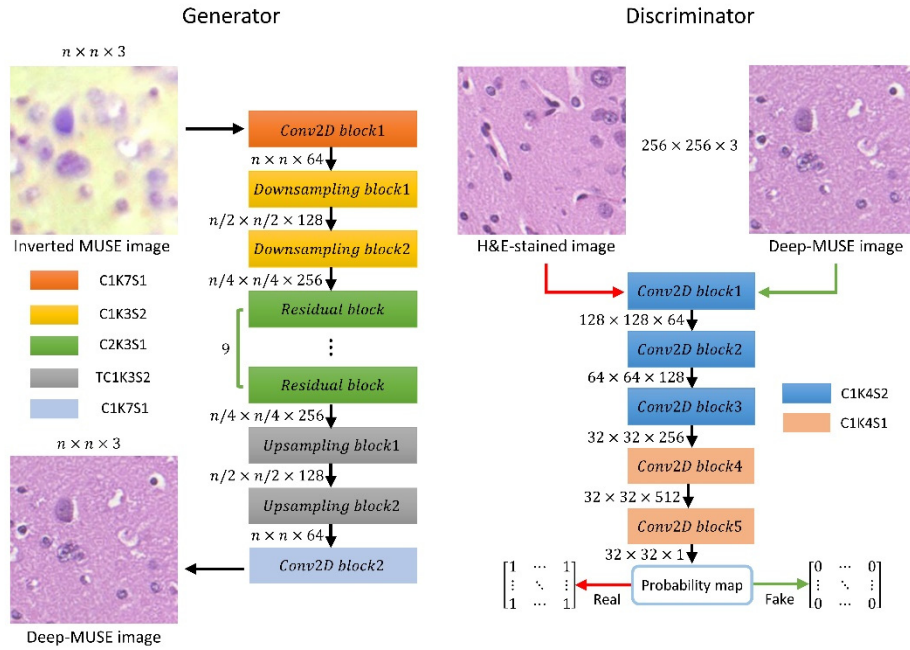


Fig. S3. The network architecture of the pix2pix and CycleGAN models. (A) The pix2pix model uses paired images for training. (B) The network architecture of the generator and the discriminator in both pix2pix and CycleGAN models. The tensor size of the input, intermediate, and output is represented by *Height* \times *Width* \times *Channel*, e.g., $256 \times 256 \times 3$ denotes the RGB image with a pixel number of 256×256 . The color blocks have different structures and parameters, e.g., C1K7S1 denotes the block has 1 convolution layer with 7×7 kernel size and stride 2, TC1K3S2 denotes the block has 1 transposed convolution layer with 3×3 kernel size and stride 2.

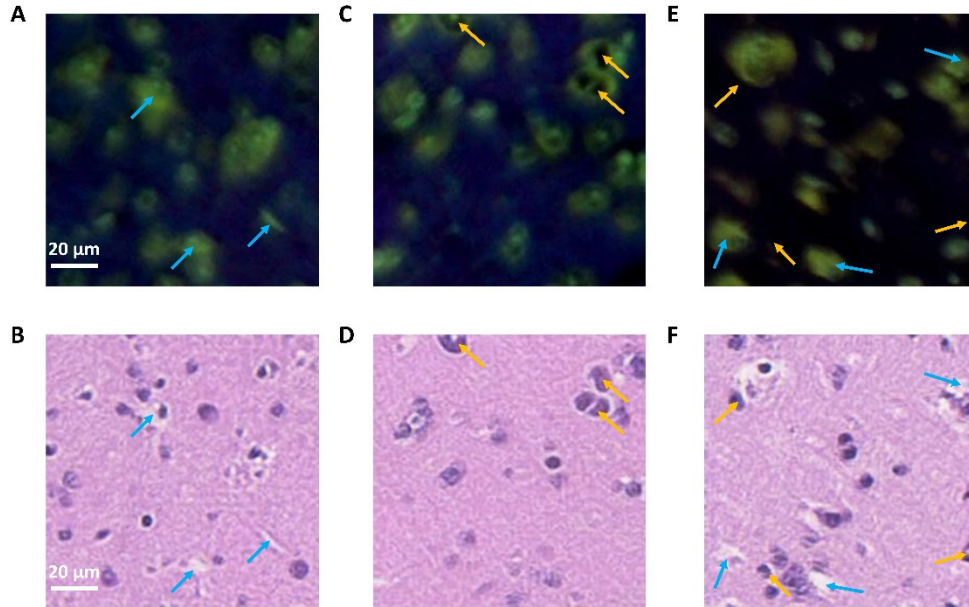


Fig. S4. Unsatisfactory style transformation of CycleGAN model training with original MUSE images without flipping contrast. (A, C, E) Three MUSE images of FFPE mouse brain slices. (B, D, F) The Deep-MUSE images output by the CycleGAN model, corresponding to (A), (C), (E), respectively. The blue arrows show that the green cell nuclei in the MUSE images (A), (E) are converted into a white background in the Deep-MUSE images (B), (F). The orange arrows show that the black background in the MUSE images (C), (E) is converted into purple cell nuclei in the Deep-MUSE images (D), (F).

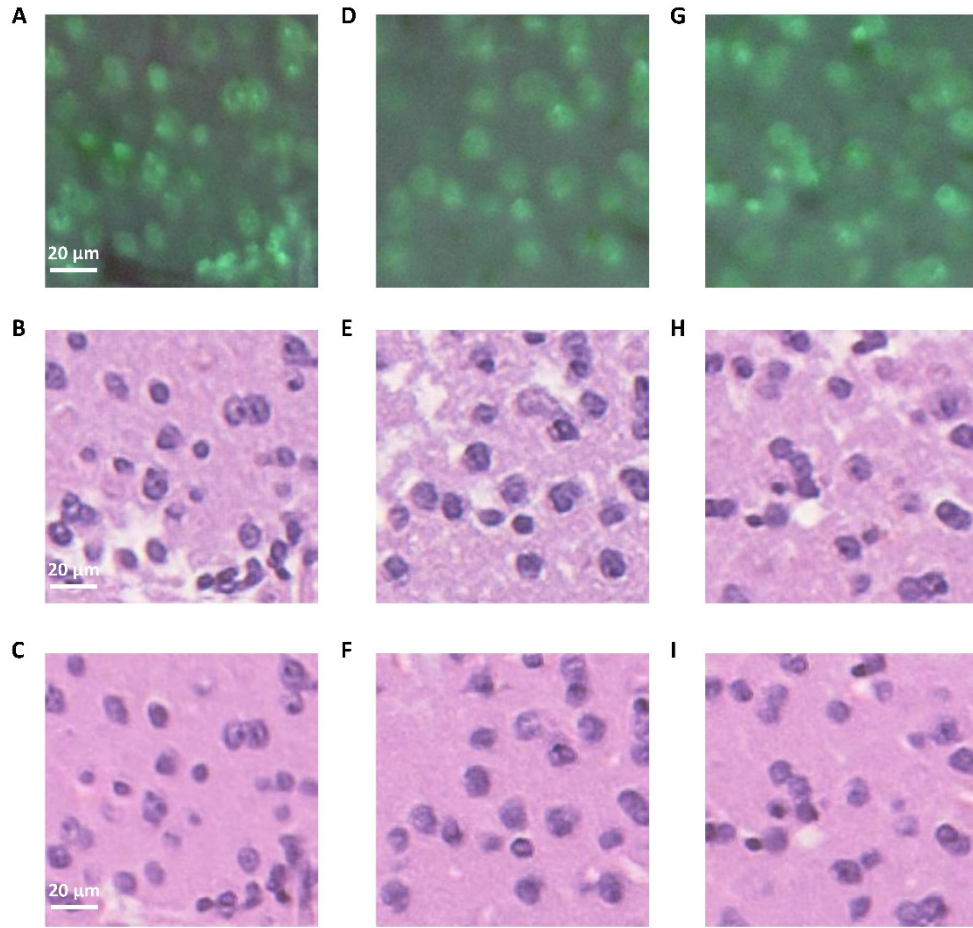


Fig. S5. Comparison between Deep-MUSE images generated by the CycleGAN model without/with SSIM loss. (A, D, G) Three MUSE images of a fixed mouse brain section. (B, E, H) The Deep-MUSE images output by the CycleGAN model trained without SSIM loss, corresponding to (A), (D), (G), respectively. (C, F, I) The Deep-MUSE images output by the CycleGAN model trained with SSIM loss, corresponding to (A), (D), (G), respectively.

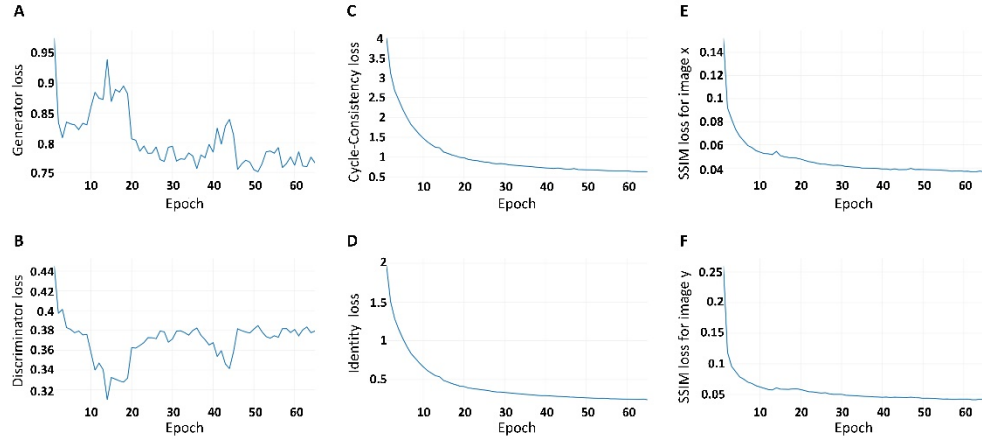


Fig. S6. Training loss curves of the CycleGAN model. (A) Generator loss curve of the generators G and F . (B) Discriminator loss curve of the discriminators D_X and D_Y . (C) Cycle consistency loss curve. (D) Identity loss curve. (E) SSIM loss curve of image domain X . (F) SSIM loss curve of image domain Y .

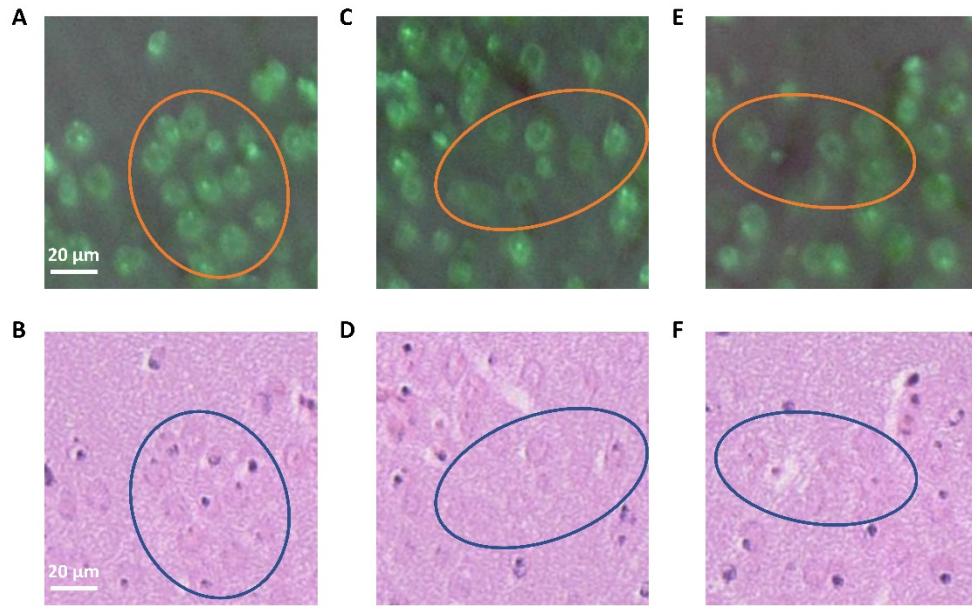


Fig. S7. Unsatisfactory style transformation by testing MUSE images of the thick tissue on a well-trained pix2pix model for FFPE thin slices. (A, C, E) Three MUSE images of a fixed and thick mouse brain. (B, D, F) The Deep-MUSE images output by the pix2pix model, corresponding to (A), (C), (E), respectively. The blue circles in (B), (D), (F) show the missing cellular structures compared with the orange circles in (A), (C), (E).

Visualization 1. Closeup images of a column in the ROI of an FFPE mouse brain section acquired by MUSE, which are compared with their corresponding H&E-stained images using different methods. The 5X close-up scanning window with a pixel number of 500×500 ($\sim 221 \times 221 \mu\text{m}^2$). The images of different columns (from left to right) represent MUSE images, Deep-MUSE images by the pix2pix model, Deep-MUSE images by the CycleGAN model, and ground truth H&E-stained images.

Visualization 2. Closeup images of a column in the ROI of a fixed and thick mouse brain sample acquired by MUSE, which are compared with their corresponding Deep-MUSE images and the H&E-stained images of the adjacent layer. The 5X close-up scanning window with a pixel number of 500×500 ($\sim 224 \times 224 \mu\text{m}^2$). The images of different columns (from left to right) represent MUSE images, Deep-MUSE images by the CycleGAN model, and reference H&E-stained images of the adjacent layer.